Analysis of Noncovalent Complexes of DNA and RNA by Mass Spectrometry

Steven A. Hofstadler and Richard H. Griffey*

Ibis Therapeutics, a division of Isis Pharmaceuticals, 2292 Faraday Avenue, Carlsbad, California 92008

Received March 28, 2000

Contents

I. Introduction

Nearly 10 years ago, Ganem et al. published a seminal work demonstrating that a noncovalent complex between FK binding protein (M_w 11 812 Da) and the ligand FK506 could be transported intact from solution into the gas phase using electrospray ionization (ESI) and detected using mass spectrometry (MS).[1] While the value of ESI-MS for the ionization of intact large biopolymers had been demonstrated two years earlier,[2] the validity of their work and the utility of ESI-MS for characterization of noncovalent complexes in a broad range of chemical and biological applications was unappreciated at the time. Further, many in the mass spectrometry community were skeptical as to whether noncovalent complexes observed using ESI-MS truly reflected the solution populations of the same complexes or were merely artifacts created during the evaporation of solvent and buffer from ions in the charged electrospray plume. Despite the limitations of the early instrumentation, these researchers and others detected noncovalent complexes between nucleic acids, proteins, and small molecules and studied the gas-phase conformations of the ions as a function of both solution and ESI-MS conditions.[3,4]

The utility of ESI-MS for the ionization, detection, and characterization of noncovalent complexes of nearly every type of biomolecule has now been described in ~300 publications and more than 20 review articles.[5−8] Mass spectrometry has a major advantage over other biophysical tools: the identities and abundances of different complexes can be determined from direct observation, since the mass of every molecule serves as the intrinsic detection "label". ESI-MS has been used to characterize various features of protein−protein, protein−DNA, protein−RNA, and DNA−DNA complexes including macromolecular and ligand binding stoichiometry and solution binding affinities. Molecular interactions with dissociation constants ranging from nanomolar to millimolar can be characterized using ESI-MS. Once isolated in the gas phase, noncovalent complexes can be interrogated via dissociation (MS/MS) to determine binding sites or can be probed for structural features using ion−molecule reactions (such as hydrogen−deuterium exchange).

This review highlights the power of ESI-MS for characterization of noncovalent complexes of nucleic acids. These include DNA and RNA duplexes, triplexes and quadruplexes, interaction of DNA and RNA with proteins, and complexes between nucleic acids and small molecule ligands. Applications in the latter area have impacted drug discovery efforts against structured RNAs, an important but unexploited class of macromolecular target.[9] The unique capabilities of ESI-MS relative to other analytical methods are highlighted. These include exploration of atypical solution conditions for the determination of dissociation constants, target discrimination among multiple ligands under competitive or noncompetitive binding conditions, parallel binding of multiple ligands to multiple targets, observation of two ligands simultaneously binding to a single target, and identification of ligand binding sites using rapid mass spectrometry-based protection assays. We have not discriminated among MS platforms during the discussion unless instrument performance was particularly enabling or limiting. Mass spectrometry also has great utility in determining the primary sequence of nucleic acids, a subject covered in various reviews.[10−12] We have limited the scope of this review to ESI-MS of noncovalent complexes containing one or more oligonucleotide. Studies employing other ionization techniques such as matrix-assisted laser desorption ionization (MALDI) are outside the scope of this review, and the reader is referred to the literature for other topical reviews.[13−16]

10.1021/cr990105o CCC: $36.00
Published on Web 01/18/2001

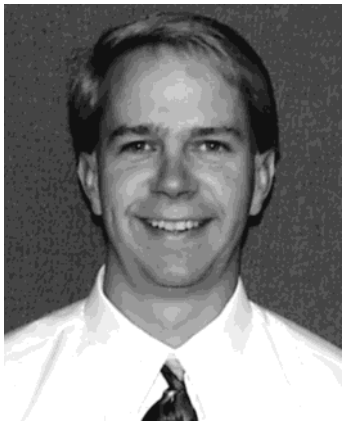

Steven A. Hofstadler received his B.S. degree in Chemistry from the University of New Mexico in 1988 and his Ph.D. degree in Analytical Chemistry from The University of Texas at Austin in 1992. Upon completing his graduate studies, he worked as a Postdoctoral Research Fellow at Pacific Northwest National Laboratory, where he developed high-performance instrumentation and methodologies based on Fourier transform ion cyclotron resonance (FTICR) mass spectrometry. Upon completion of his postdoctoral studies, he remained at Pacific Northwest National Laboratory as a Senior Research Scientist for nearly five years, during which time he continued to develop FTICR instrumentation in combination with numerous microcolumn separations. In 1997 Dr. Hofstadler relocated to Isis Pharmaceuticals, Inc., where he is presently an Executive Director in the Ibis drug discovery division. His most current research interests are centered around applications of FTICR MS for the characterization of noncovalent complexes between RNA and small drug-like molecules.

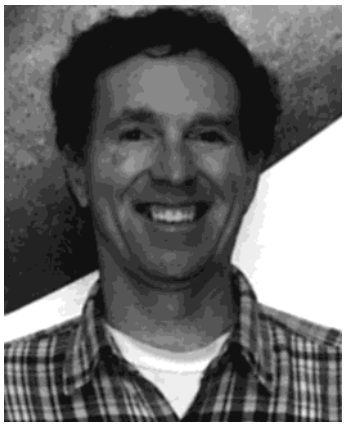

Dr. Griffey is the Vice President of Research for Ibis Therapeutics. He obtained his B.A. degree in Chemistry from Rice University (1978) and his Ph.D. degree in Chemistry from the University of Utah (1983) under the direction of Professor C. Dale Poulter. Following an NIH postdoctoral fellowship with Professor A. G. Redfield, Dr. Griffey was Associate Professor of Cell Biology in the University of New Mexico School of Medicine. Dr. Griffey joined Isis Pharmaceuticals in 1991 and co-founded Ibis Therapeutics in 1997.

II. Nucleic Acid Complexes

A. DNA Duplexes

DNA duplexes have long been an attractive model system for ESI-MS studies of noncovalent complexes. Multiply charged duplex ions are stable in the gas phase for extended periods, even with unsolvated charges. Their gas-phase stability is balanced between the number of hydrogen bonds and base stacking among the nucleobases and the total charge present on the strands. Duplex ions with lower charge states are more stable and may retain structures similar to their solvated solution counterparts.

Light-Wahl et al.[17] showed that ions from a 20mer DNA duplex could be detected using ESI-MS, with charge states distributed from $[M - 2H^+]^{2-}$ to $[M - 8H^+]$.[8] Ganem and co-workers demonstrated that the relative abundance of ions from the duplex relative to the single strands was increased for a GC-rich 8mer compared to an AT-rich 8mer duplex.[18] They attributed this difference to enhanced solution stability for the GC-rich duplex at the ESI interface. Collisional activation and MS/MS performed on the $[M - 3H^+]^{3-}$ charge state of the AT 8mer duplex with a triple-quadrupole instrument at low collision energies produced $[M - 2H^+]^{2-}$ single strands without fragmentation of the strands.

An important early study on the detection and reactivity of ions from DNA duplexes using a quadrupole ion-trap mass spectrometer was reported by Doktycz et al.[19] They demonstrated that 20mer and 10mer duplexes were stable for hundreds of milliseconds in the gas phase under the multiple ion−molecule collision conditions present in the ion trap and did not require solvation to maintain a stable duplex. In addition, duplex ions remained intact during activation and resonance ejection from the ion trap. Preliminary observations suggested that the duplex could be collisionally dissociated in the gas phase via resonance excitation.

Bayer et al. denatured DNA duplexes in solution by addition of triethylamine and showed that duplex ions were not observed using ESI-MS. They generated ions from conjugated DNA duplexes, phosphorothioate DNA duplexes, and phosphodiester DNA duplexes. Changes in the charge state distribution of the duplex ions were observed when the length of one strand was varied.[20] Greig et al. studied the charge state distribution for DNA:DNA and DNA:PNA duplexes as a function of electrospray ionization conditions.[21] They noted an increase in intensity from duplex ions relative to the single strands at lower flow rates which correlated with the "harshness" of the ESI process. Cheng et al. measured the relative solution stability of unnatural 2′−5′-linked DNA:DNA duplexes and DNA:DNA duplexes from the stoichiometry of binding between the strands.[22]

A mass spectrum acquired on an ESI Fourier transform ion cyclotron resonance (FTICR) mass spectrometer of a 13 base pair DNA duplex mixed with a noncomplementary 12mer single strand is presented in Figure 1. The solution contained 150 mM ammonium acetate buffer, pH 7.0. Thirty three percent isopropyl alcohol was added to aid the electrospray desolvation. Two 13mer DNA strands (5′-GCCCAAGCTGGCA ($MW_{monoisotopic}$ = 3942.705 Da) and 5′-TGCCAGCTTGGGC ($MW_{monoisotopic}$ = 3964.688 Da), 5μM each) were mixed with a 12mer DNA 5′-GGCGGTACGTGC ($MW_{monoisotopic}$ = 3700.648 Da) (5 μM). The major signals are generated by the $[M - 5H^+]^{5-}$ ions from the 13mer DNA duplex at *m/z* 1580.471 (monoisotopic) and the $[M - 3H^+]^{3-}$ ions from the unpaired single-strand DNA at *m/z* 1232.540 (monoisotopic). No signals are detected from nonspecific duplex ions generated by the 12mer DNA paired with either 13mer strand (BX or BY in the insert) nor are any signals detected which are consistent

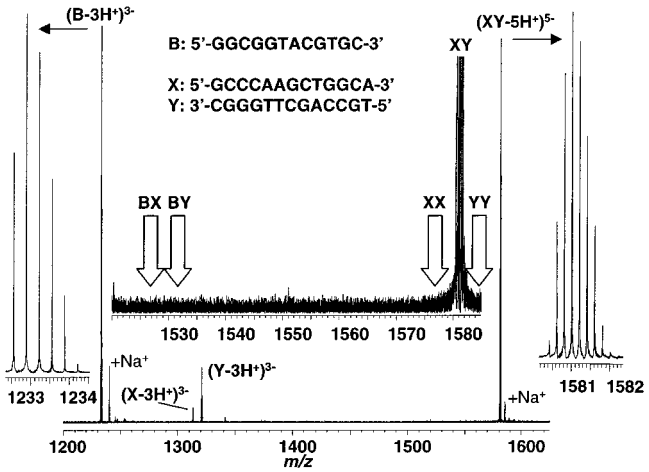

Figure 1. Specificity of DNA duplex formation in solution monitored using ESI-FTICR-MS. Signals are observed from $[M - 3H^+]^{3-}$ ions of the unbound single-strand 12mer at *m*/*z* 1232.540 and from the $[M - 5H^+]^{5-}$ (monoisotopic) ions of the 13 base pair duplex at *m*/*z* 1580.417. Weaker peaks are generated by the respective ions with one adducted sodium ion and from ions generated by the X and Y single strands (*m*/*z* 1312−1325). No signals are observed corresponding to the nonspecific BB, BX, BY, XX, or YY duplexes (central insert). In addition, the high mass resolving power of the FT-ICR mass spectrometer allows unambiguous assignment of the charge state for each species present in solution (left and right inserts). The average mass resolution shown for the single-strand and duplex species is 320 000 and 260 000 (FWHM), respectively.

with nonspecific homoduplex ions (from XX, YY, or BB duplexes). Hence, the solution specificity of binding is maintained into the gas phase during the desolvation of the duplex and single strand. The high resolving power afforded by the ESI−FTICR MS platform (e.g., in Figure 1, $M/\Delta M > 260\,000$ for the duplex ions and $M/\Delta M > 320\,000$ for the single strand) provides direct charge (and thus mass) determination for molecular and fragment ions concurrent with low or sub-ppm mass measurement error. Solutions containing 5 mM ammonium acetate that disfavor duplex formation produce signals from the respective single strands. The mass resolution and accuracy obtained with the FT-ICR mass spectrometer limit the base composition of each strand to a single possibility. As noted by Aaserud et al. and by Muddiman et al., knowledge of base composition from measurement of exact mass can be used to identify the origin of PCR products.[23,24]

Mass analysis of longer (60−500 base pair) duplex DNA anions generated by PCR has demonstrated utility in the taxonomic classification of microorganisms. Naito et al. first measured the masses of two 91mer DNA strands generated from the APC gene using PCR under denaturing ESI-MS conditions.[25] Subsequently, Wunschel and co-workers showed that duplex ions from PCR reactions could be observed intact and that measurement of molecular mass limited the possible lengths of the products.[26] Aaserud et al. noted that very accurate (<1 Da) FT-ICR MS measurement of the masses of double-stranded DNA up to 39 kDa along with measurement of the masses of the respective single-strand ions greatly limits the possible base compositions of the respective strands.[23] Additional sequence information obtained from MS/MS experiments further eliminated many of the possible base compositions. Muddiman et al. demonstrated that mass tags incorporated onto individual bases of the duplex further constrained the possible base compositions to one solution in a 114 bp PCR product.[24] Masses of even larger DNA duplexes (500 base pairs) have been measured with 87 ppm accuracy using ESI−FTICR MS.[27] Studies of large DNA duplexes are limited by the reduction in signal-to-noise produced by the natural distribution of ^{13}C and ^{15}N, difficulties in measurement of the average molecular mass, and generation of multiple product strands by some polymerases. Incorporation of isotopically depleted nucleotides should facilitate identification of nucleotide substitutions, additions, or deletions, critical for genotyping applications.

Finally, it is worth noting that much larger DNA molecules have been successfully promoted into the gas phase using ESI. Cheng and co-workers trapped individual ions from a 1.95 MDa pGEM-5S plasmid DNA in an FTICR instrument, reacted them with acetic acid to observe charge state shifting, and calculated a molecular weight to within 0.3%.[28] Chen et al. trapped single ions from T4 DNA using ESI−FTICR MS and observed charge state shifting during a 476 s transient.[29] An ionic mass of 110 MDa was obtained by direct measurement of the number of charges carried by individual ions.

1. Duplex Structure

Studies on the gas-phase stability and structure of DNA duplexes are of interest from a physical and biochemical perspective. The solution stability of duplex DNA is attributed to a variety of factors, including hydrogen bonding between the bases, the screening of backbone charge by solvent, and the stacking of the bases in the hydrophobic interior of the helix. In the gas phase, the latter two stabilizing features may be reduced or unavailable while the strengths of hydrogen bonds are increased. Although duplex ions have been observed for seven years, the nature of interaction between strands in the gas phase remains a major unanswered question.

2. DNA Duplex MS/MS

McLafferty and co-workers studied the infrared multiphoton dissociation (IRMPD) of 64 and 70 bp duplex DNA ions.[30−33] Initial short laser heating of the duplex ions boiled off noncovalently associated water and ammonium ions. Increasing the IRMPD energy produced fragment ions from the termini of the respective single strands which could be assigned based on exact mass or the complementary sequence. IRMPD activation yielded more fragment ions than blackbody irradiation or nozzle-skimmer dissociation. Extensive fragmentation at internal sites of each strand were observed. Nearly complete sequence could be obtained for the 64mer duplex. Gabelica et al. studied the collisionally activated dissociation (CAD) of a 12mer DNA duplex. Using a qTOF instrument, they observed that the capillary-skimmer voltage difference required to dissociate 50% of the $[M - 5H^+]^{5-}$ duplex ions was higher than for the $[M - 6H^+]^{6-}$ ions.[34] A difference in the charge state

of the resulting single strands was noted and attributed to differences in the solution pK_as of the bases on each strand. Wan and co-workers performed CAD of a self-complementary 12mer DNA duplex using an ion-trap mass spectrometer.[35] They observed both dissociation of the duplex into the resulting single strands and loss of neutral bases from the intact duplex ions. Schnier et al. studied the dissociation of DNA duplex ions using blackbody infrared radiative dissociation (BIRD) in an FT-ICR mass spectrometer.[36] Their study reported many intriguing results, including unusually high solution stability for a seven base pair AT duplex in 50% acetonitrile. BIRD dissociation of ions from a seven base pair GC duplex yielded only fragment ions rather than strand dissociation as observed for ions from an AT duplex. They concluded that the calculated differences in activation energy and fragmentation of noncomplementary duplexes compared to complementary duplexes were consistent with hydrogen bonding between strands in the gas phase.

We have studied the gas-phase dissociation and fragmentation of duplex ions and duplex ions containing base pair mismatches.[37] In the gas phase, collisional activation of ions from short DNA duplexes (8−12 base pairs) results predominantly in strand dissociation. However, collisional activation of longer duplex ions induces fragmentation of both strands. If the strands have unique sequences, the locations of the internal fragmentation of the duplex ions can be ascertained from the *m*/*z* of the fragment ions. This strategy has been used to monitor the change in gas-phase ion structure induced by base pair mismatches. Two RNA−DNA duplexes were generated by co-mixing an RNA 14mer with a complementary DNA strand and a second DNA strand containing a dG→dA mutation. The RNA strand is relatively refractory to fragmentation at energies where the DNA strand fragments.[38] Simultaneous MS/MS on the $[M - 5H^+]^{5-}$ charge state of both duplexes resulted in preferential fragmentation of the DNA strand in the mismatch duplex, while the ions from the complementary duplex were unaffected. Analysis of the product ions from the MS/MS experiment demonstrated that fragmentation occurred predominantly at the site of the mismatch and the adjacent base pairs. CAD of a 14mer DNA:DNA duplex (Figure 2a) produces w and a-base fragment ions (nomenclature of McLuckey[39]) from both strands, with the w_4 ion of the upper strand being the most abundant fragment. Introduction of a G−G mismatch base pair for the Watson−Crick G−C base pair alters the fragmentation pattern observed at the same collisional activation energy. As shown in Figure 2b, the w_4 fragmentation channel for the upper strand is retained while three new w ion sites of fragmentation are introduced adjacent to the mismatch pair. In addition, two new w ion fragments are observed on the lower strand while two w ion fragments from the 3′-terminus are reduced in intensity. Ion intensities from several fragmentation pathways are attenuated. These results suggest that gas-phase cleavage is directed toward structural defects in the double strand generated by the mismatched base pairs.

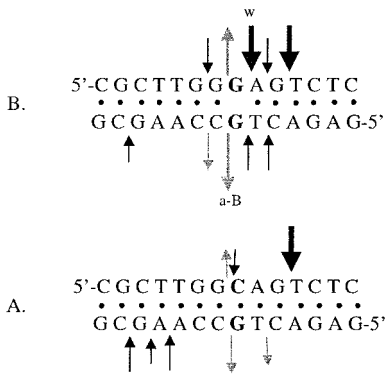

Figure 2. Collisionally activated dissociation of DNA duplexes. (A) Complementary duplex. (B) Duplex containing a G:G mismatch base pair. The positions of w series fragment ions are represented by arrows pointing toward the strand, while positions of a-base fragment ions are represented by arrows pointing away from the strand. The magnitude of the arrow is proportional to the abundance of the fragment ion in the spectrum.

3. DNA Duplex H/D Exchange

In solution, the labile amino, imino, and hydroxyl protons of DNA and RNA exchange with water very rapidly (milliseconds) due to rapid opening of the Watson−Crick base pairs, the high local concentration of water, and general acid/general base catalysis of the exchange process. However, in the gas phase, exchange of the labile protons is slowed dramatically. The rate of gas-phase H/D exchange of oligonucleotide anions has been shown to be a function of the reagent used for exchange, concentration of the reagent, charge state of the oligonucleotide, gas-phase basicity/acidity of the nucleotides, and internal structure of the oligonucleotide ions.[40−42]

Greig et al. studied the gas-phase H/D exchange of ions from duplex DNA and DNA:RNA heteroduplexes.[43] The observed that H/D exchange rates for duplex DNA anions were >10-fold slower than the rates observed for the respective single strands. The exchange profile showed an initial rapid period of exchange followed by a prolonged period of pseudoexponential uptake. Only 78% of the labile protons were exchanged after 15 min of reaction with 10^{-7} Torr D_2O in the FTICR cell at 9.4 T. This may result from different populations of ions with different internal structures that exchange hydrogens at different rates, differences in the exchange rates for some classes of protons, or a combination of these effects.

Hofstadler and co-workers developed a unique scheme for increasing the rate of H/D exchange at higher reagent gas pressures and extended storage times in a multipole ion storage device.[44] They demonstrated no scrambling of the incorporated deuterium upon IRMPD of partially exchanged ions. An example of H/D exchange from D_2O into single-strand and duplex ions is presented in Figure 3. The $[M - 3H^+]^{3-}$ ions from a single-stranded DNA 12mer exchange between 1 and 16 hydrogens (38 possible) after 15 s, with a normalized mole fraction of 8.9 exchanges, shown in Figure 3a. There is no population of ions that undergoes few H/D exchanges, as observed previously. The $[M - 5H^+]^{5-}$ ions from a 13 base pair duplex undergo only 2−25 H/D ex-

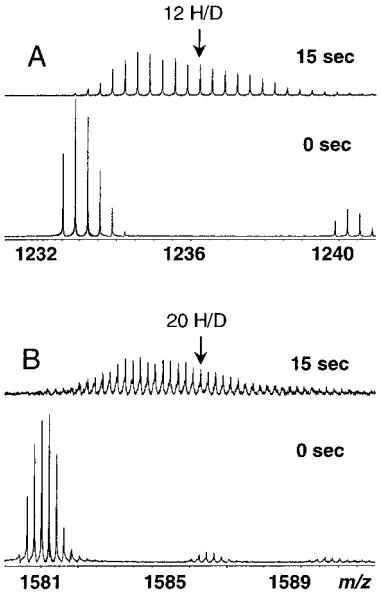

Figure 3. Time course of H/D exchange between D_2O and DNA anions. (A) $[M - 3H^+]^{3-}$ ions from 12mer single-strand DNA. (B) $[M - 5H^+]^{5-}$ ions from a 13 base pair duplex. A D_2O pressure of 1.2×10^{-5} mbar was employed in both studies, and H/D exchange was allowed to occur in the hexapole storage region for the indicated time.

changes (80 possible) after 15 s, with a normalized mole fraction of 15.5 exchanges (Figure 3b). The labile protons of the more structured duplex ions appear to be protected from H/D exchange, consistent with extensive internal Watson−Crick hydrogen bonding among the base pairs. However, a great deal of work is needed to further characterize the structure and dynamics of duplex ions in the gas phase.

B. DNA Triplexes and Quadruplexes

Higher order complexes of DNA also have been observed using negative-ion ESI-MS. Griffith and co-workers studied the binding of various peptide nucleic acids (PNAs) with a 15mer DNA strand.[45] They observed that a T,C-rich 10mer PNA strand bound to the A,G-rich DNA strand as the triplex at equilibrium. No duplex ions were observed despite a very slow on-rate for triplex formation. A bis-PNA containing a five amino acid linker bound to the DNA strand in a 1:1 complex as measured with ESI-MS. This result was consistent with formation of an antiparallel Watson−Crick duplex by one PNA strand and triplex formation by a parallel PNA strand. The binding of two PNA strands to a longer DNA did not reduce the observed charge state of the ions for the complex compared to the DNA, suggesting that the PNAs did not bind in the protonated form to an appreciable extent.

Goodlett and co-workers studied the ESI-MS stability of a noncovalent, four-stranded oligonucleotide, $d(CGCG_4GCG)_4$.[46] Ions from the quadruplex were detected from a 10 mM sodium phosphate buffer containing 0.1 mM ethylenediaminetetraacetic acid at a low nozzle-skimmer bias (−150 V) but not with a higher bias (>−250 V) corresponding to more harsh desolvation conditions. In contrast, when the sample was desalted and analyzed by ESI mass spectrometry at a low bias, only ions for the single-stranded $d(CGCG_4GCG)$ species were observed. These data agree with spectroscopic evidence which showed that oligonucleotides with the sequence motif 5′d(CGCG-(n)GCG)3′, where $n = 2-5$, formed stable four-stranded complexes in the presence of monatomic cations, like K^+, Ca^{2+}, Na^+ and Li^+, but not in their absence.

C. DNA–Protein Complexes

Many key biological functions, including DNA repair and replication, transcription and translation, and control of gene expression are regulated by specific DNA-protein interactions. Thus, probing at a molecular level how specific proteins interact with nucleic acids is key to furthering our understanding of all biological systems. ESI-MS has been used to study a number of DNA−protein complexes to probe solution phase binding stoichiometry, to explore the specificity of oligonucleotide-protein binding, and to characterize the affinity of DNA (and RNA) binding proteins for their oligonucleotide target sequences.

Early work by Griffey and co-workers employed ESI-MS to study the binding of a 20-mer phosphorothioate oligonucleotide to bovine serum albumin (BSA).[47] In that work, relative levels of free and bound oligonucleotide were determined by the signal intensities in the mass spectrum. By holding the BSA at a fixed concentration and measuring the ratio of free/bound oligonucleotide at varying initial oligonucleotide concentrations, K_D values for the BSA−oligonucleotide complex were determined. The mass spectra revealed that under the conditions employed, BSA could bind two oligonucleotides. The relative amount of bound/free BSA was plotted against the initial oligonucleotide concentration and fit to a second-order polynomial. From these measurements it was determined that the two oligonucleotide binding sites have macromolecular dissociation constants of $3.1 + 0.3\ \mu M$ (K_{D1}) and $11.9 + 0.6\ \mu M$ (K_{D2}) at pH 7.5. Furthermore, the value of K_{D1} was found to be sensitive to the ionic strength of the buffer, suggesting that electrostatic forces contribute significantly to the binding energy of the complex. These K_D values were further corroborated by capillary electrophoresis measurements, which yielded values in good agreement with those obtained by ESI-MS. Subsequent work by the same group demonstrated a strong correlation between the in-vivo pharmacokinetic properties of a collection of phosphorothioate oligonucleotides and their respective MS-derived K_D.[48] While albumin is not generally regarded as a specific "DNA binding protein", the authors clearly demonstrated that ESI-MS measurements of oligonucleotide−protein complexes can be exploited to measure binding constants and binding stoichiometry.

After the Griffey K_D paper was published, a number of papers were published demonstrating that noncovalent complexes between size-specific and sequence-specific DNA binding proteins could be transferred to the gas-phase intact and that complexes observed in the gas phase correlated with known solution-phase binding specificity and stoichiometry. For example, Cheng and co-workers used

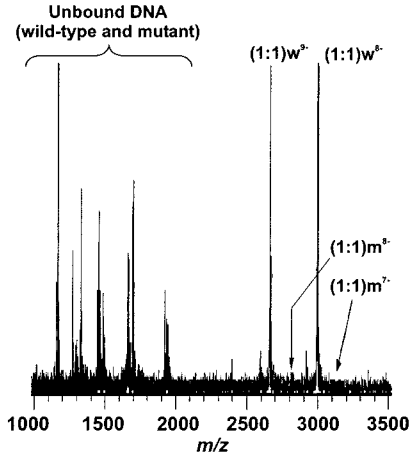

Figure 4. ESI mass spectrum of 5 μM PU.1 binding protein in the presence of 15 μM "wild-type" 17 base pair duplex containing the GGAA recognition sequence and 20 μM "mutant" 19 base pair duplex which lacks the recognition sequence. Complexes are observed only between PU.1 and the wild-type DNA, while no complexes are detected for PU.1 binding to the mutant DNA despite the fact that it is present in greater molar excess. Complexes with the wild-type DNA are denoted as (1:1)w^{n-}; arrows indicate the position where the putative mutant complexes, (1:1)m^{n-}, would fall. (Adapted with permission from ref 49. Copyright 1996 Academic Press.)

ESI-MS to explore the binding properties of a 13.5 kDa construct of the DNA binding domain of the double-strand DNA binding protein PU.1 (also referred to as Spi1).[49] PU.1, like other eukaryotic transcription factors, recognizes the nucleotide sequence GGAA/T and binds to dsDNAs containing the recognition sequence with a 1:1 stoichiometry. The specificity of PU.1 for double-stranded DNA containing the recognition sequence was evaluated in an ESI-MS-based competitive binding assay. In that work the only noncovalent complexes observed from ESI-MS of a solution containing PU.1, a 17 bp duplex containing the GGAA recognition sequence ("wild type"), and a 19 bp duplex in which the central GGAA moiety was replaced with a GCTA ("mutant") corresponded to the PU.1-wild-type DNA. It was noted that in addition to an extra T on the 5′ end, the only difference between the wild-type sequence (5′-TGAAAGA***GGAA***CTTGGT-3′) and the mutant sequence (5′-***T***TGAAAGA***GCTA***CTTGGT-3′) was a two base mutation at the recognition site. As shown in Figure 4, even when the mutant sequence was present in excess relative to the wild-type sequence, only complexes between the wild-type sequence and PU.1 were observed. On the basis of a signal-to-noise ratio of 10 for the wild-type protein-PU.1 complex, the authors concluded that a difference in binding affinity of >200 was observed. A gel shift assay employing ^{32}P-radiolabeled dsDNA (wild-type and mutant) confirmed the high affinity of PU.1 for the wild-type construct and the lack of formation of a PU.1-mutant complex, even in the presence of a significant excess of mutant DNA.

Subsequent work by the same group used ESI-MS to explore the binding stoichiometry of the single-stranded DNA binding protein gene V.[50,51] Unlike PU.1, gene V from the bacteriophage f1 does not recognize a specific sequence from a double-stranded DNA; instead, it binds to and stabilizes single-stranded DNA during phage replication. Gene V also binds selectively to the 5′ operator sequence of the gene II mRNA of phage f1 and represses the translation of the gene II protein. Gene V represents a unique model system with which to study noncovalent complexes by mass spectrometry. Under physiological solution conditions, gene V is purported to form a homodimer with a K_D of $\sim 10^{-12}$ M and it is the homodimer which is thought to bind to ssDNA. Cheng and co-workers showed that while under denaturing solution conditions only the protein monomer was observed, ESI-MS from a 10 mM NH_4OAc solution at pH 7 yielded exclusively the protein homodimer. Binding between the gene V dimer and ssDNA targets of varying length was used to probe binding stoichiometry. As later confirmed by size exclusion chromatography, a length-dependent binding stoichiometry was observed. Oligonucleotides $\leq$15 bases in length bound the gene V dimer with a 1:1 stoichiometry, while oligonucleotides $\geq$16 bases were observed to preferentially bind the gene V dimer with a 2:1 (dimer:DNA) stoichiometry, suggesting a binding stoichiometry of eight nucleotides/dimer. Previous (nonmass spectrometric) studies of the gene V system indicated a binding stoichiometry of 3−5 nucleotides for each protein monomer (i.e., 6−10 nucleotides/dimer), but it could not be unambiguously determined whether the measured stoichiometry represented the average of a range of binding stoichiometries or a single, quantized binding stoichiometry. The data presented in this work provide strong support to the hypothesis that the gene V "footprint" covers eight nucleotides per homodimer.

A number of other studies in which ESI-MS was employed to study specific protein−DNA noncovalent complexes have been published in recent years; each paper provides additional insight into the solution conditions and instrumental parameters required for effective analysis. For example, Veenstra and co-workers used ESI-MS to study the zinc-dependent binding of the DNA-binding domain of the vitamin D receptor (VDR DBD) to the vitamin D response element (VDRE) from the mouse osteopontin gene.[52] ESI-MS measurements made it possible to count the number of Zn^{2+} ions bound to the VDR DBD protein and to correlate the formation of the protein−DNA complex with the Zn-adducted state of the protein. It was shown that at 100 μM Zn^{2+} (the concentration at which the protein bound primarily two Zn^{2+} ions), optimal complex formation was observed, while at higher Zn^{2+} concentrations (at which higher order Zn^{2+} binding was observed) the complex was significantly dissociated.

Another study in which protein−DNA noncovalent complexes were analyzed by mass spectrometry was that of Potier and co-workers in which the *trp* repressor−DNA complex was studied using ESI-TOF MS.[53] In that work the *trp* apo-repressor protein was initially detected as a partially unfolded monomer. Upon addition of a 21 base pair dsDNA containing the recognition element (two symmetrically arranged CTAG recognition sequences separated by a four base pair spacer) a homodimer-dsDNA complex was ob-

served with a 1:1 binding stoichiometry. Interestingly, the tryptophan co-repressor was not needed for complex formation. Collision-induced dissociation of the complex revealed that the complex was refractory to dissociation; the collision energy required to disrupt the complex was approximately equivalent to that needed to dissociate covalent bonds. DNA binding specificity was explored by preparing three DNA constructs with two, four, and six base pair spacers between the CTAG recognition elements. Under competitive binding conditions, only the DNA with the correct four base pair spacer formed a complex with the *trp* apo-repressor protein. Further studies probing the affinity of the protein−DNA complex for D- and L-tryptophan and 5-methyl-tryptophan showed that both 5-methyl- and L-tryptophan bind to the complex with high affinity and specificity while both the affinity and specificity of D-tryptophan binding is significantly reduced.

Finally, Xu and co-workers recently reported ESI-FTICR-MS studies of the minimal binding domain of xeroderma pigmentosum group A complementing protein (XPA) with cisplatin-adducted oligonucleotides.[54] High-resolution FTICR-MS measurements revealed that XPA bound to undamaged and "damaged" (i.e., cisplatin adducted) 20-mer duplexes with comparable affinity−only a slight preference for the "damaged" DNA was observed. These finding were contrary to previous studies employing a 258-bp DNA substrate which suggested a significant difference in affinity of XPA for damaged and wild-type DNA. The observed binding stoichiometry was 1:1 for the undamaged dsDNA, while both 1:1 and 2:1 (protein:DNA) binding stoichiometry was observed for the damaged dsDNA.

D. RNA–Protein Complexes

Whereas a number of DNA−protein systems have been interrogated by ESI-MS, the use of ESI-MS to study RNA−protein complexes has been rather sparse—likely due in part to the inherent difficulties associated with RNA handling and the ubiquitous nature of RNA nucleases. As described below, a few macromolecular complexes containing RNA (such as ribosomal subunits and viruses) have been studied by ESI-MS, but at the time of this writing, only a few instances of ESI-MS studies of RNA−protein complexes appear in the literature. Sannes-Lowery and Loo and co-workers published a number of papers in which ESI-MS was used to study the interaction between the human immunodeficiency virus (HIV) Tat peptide and the viral transactivation responsive (TAR) RNA element.[55−59] Their first paper examined the binding of both full length Tat protein and smaller Tat peptides (Tat_{40}) to a series of TAR RNA constructs.[55] Consistent with gel mobility shift assays, a binding stoichiometry of 1:1 was observed for the Tat_{40}−TAR complex in both the positive and negative ionization modes. At a significant molar excess of Tat_{40}, additional (presumably nonspecific) binding of a second and a third Tat was observed. A number of mutant TAR RNA constructs were prepared in which essential structural elements, such as the three base bulge and the six base loop, were deleted. The binding of these constructs to Tat was evaluated under competitive and noncompetitive conditions. Consistent with solution-phase studies, it was observed that the UCU bulge of TAR RNA is a key element for Tat binding. Competitive binding experiments between a 31-mer wild-type TAR RNA and 28-mer "bulgeless" RNA revealed that the affinity of the Tat_{40} peptide was significantly reduced for the RNA construct without the bulge. Replacing the bulge with a PEG linker did not restore the high Tat binding affinity. Alternatively, consistent with previously reported structural data, it was found that deletion of the six base loop did not appreciably affect Tat affinity. As described below, subsequent work by the same group explored the use of small molecules which bind directly to the TAR RNA and serve to disrupt the Tat−TAR complex.

While the aforementioned studies are based on relatively well understood model systems, the excellent agreement between ESI-MS derived binding stoichiometries and specificities provides researchers with a growing level of confidence regarding the application of ESI-MS to study noncovalent oligonucleotide−protein complexes which are less well-characterized. Case in point, the RNA-binding protein bacteriophage T4 regA is a translational regulator which regulates the expression of as many as 30 T4 genes—including the regulation of its own mRNA. Liu and co-workers used ESI−FTICR-MS to study noncovalent complexes between regA and a family of four RNA constructs (and their degradation products).[60] The goal of the study was to correlate ESI-MS-derived relative binding affinities with those suggested by previously published in vitro repression experiments. This study was more informative, yet significantly more challenging, than the authors anticipated due to the extensive degradation of the RNA targets and the presence of multiple synthetic failure sequences. On the basis of the relative abundance of free and bound RNA, the authors observed a dramatic difference in binding between the 17-mer RNA construct derived from gene 44 and a single base-loss degradation product. Due to the extensive degradation of the gene 44 RNA target and the associated uncertainties associated with concentration of the intact target, it could not be unambiguously determined which RNA bound with the highest affinity to regA. The other three targets suffered significantly less degradation, and the authors were able to rank order their regA binding affinities in a manner consistent with previously published repression studies. A particularly novel aspect of this work was an attempt to locate the site(s) of regA-RNA interaction by sustained off-resonance irradiation (SORI) collisionally activated dissociation (CAD)[61] in the trapped ion cell of the FTICR spectrometer. A single charge state of the regA/RNA complex was selectively accumulated in the trapped ion cell and subsequently dissociated via SORI. The high resolving power and mass accuracy of the FTICR instrument allowed direct charge state, and thus mass, determination of each fragment ion based on the spacing of the isotope peaks. Fragment ions were correlated with specific regA protein fragments with

the preponderance of the fragment ions containing the amino terminus. Assuming that a portion of the protein not directly involved in RNA binding would preferentially fragment upon collisional activation, the authors concluded that the N-terminal portion of regA (up to E62) is likely not directly involved in binding the gene 44 RNA.

E. Macromolecular Complexes: Viruses, Ribosomes, and Beyond

It is now appreciated that the majority of cellular activities are mediated by mulitcomponent macromolecular complexes ("machines"). These complexes may only be stabile under physiological conditions, i.e., high concentrations of monovalent and divalent cations. Their molecular masses often exceed 1 MDa. At first glance such complexes would appear to be beyond detection using ESI-MS, but recent publications suggest that ESI-MS is well-suited for their study. Several fundamental biological complexes are comprised of a single nucleic acid strand specifically associated with a collection of proteins. For example, nonenveloped viruses consist of a single DNA or RNA molecule encased in a capsid protein coat. As the capsid is comprised of noncovalently associated protein monomers and there is no covalent attachment between the nucleic acid moiety and the capsid, a virus can reasonably be considered a macromolecular noncovalent complex. In an elegant experiment by Siuzdak and co-workers[62,63] it was shown that under the appropriate solution and interface conditions, an intact viral particle could survive the electrospray process and be transmitted through a quadrupole mass filter. Because of the limited *m*/*z* range of the spectrometer, mass spectra of the viruses were not recorded, yet a signal was detected consistent with charged viral particles striking the detector. To confirm that intact viruses were transmitted through the quadrupole sections, a collector plate was placed between the second and third quadrupoles of a modified triple-quadrupole mass spectrometer. After a solution containing intact viral particles was electrosprayed, the collector plate was removed and imaged by electron microscopy revealing the presence of intact viruses. Both tobacco mosaic virus and rice mottle virus retained their distinctive rodlike and spherical appearances, respectively. Most importantly, the tobacco mosaic virus was shown to remain viable; a tobacco leave inoculated with the collected suspension was infected by the recovered virus. Despite the limited mass spectral information derived from this early study, it clearly paved the way for other researchers to explore macromolecular noncovalent complexes on mass spectrometers with extended *m*/*z* ranges. Using a home-built ESI-TOF instrument, Chernushevich and co-workers studied a number of large noncovalent complexes and noted a linear correlation on a log−log plot of charge state vs mass.[64] Early attempts at ESI-MS analysis of the 4.7 MDa brome mosaic virus yielded a poorly resolved mass spectrum comprised of a "hump" centered around *m*/*z* 27 000; the encouraging feature of the spectrum was that the position of the hump was consistent with an average charge state of ∼175 as predicted by the log−log relationship between average charge state and molecular weight.

Recent work by Robinson and co-workers provides compelling evidence suggesting that intact viruses can be analyzed by ESI-MS.[65] Using a modified ESI-TOF instrument, mass measurements were performed on intact bacteriophage MS2 virus capsid. Bacteriophage MS2 is an icosahedral virus comprised of 180 copies of a capsid coat protein wrapped around a single 3569 base RNA molecule. Employing a nanospray ESI assembly, an aqueous pH 7.1 solution containing 5 μM virus capsid produced mass spectra with partially resolved charge states centered at ∼22 000 *m*/*z*. Charge states of +102 to +123 were assigned to the charge envelope based on an error minimization routine in which the standard deviation of the envelope was plotted over a range of putatively assigned charge states. The resulting mass measurement yielded a value of 2 484 732 ± 25 222 Da with an error of ±0.55%. Despite the fact that these measurements were performed at a slightly lower pH than those of Chernushevich and co-workers, the observed charge state distribution is in good agreement with that predicted by their derived mass to primary charge-state relationship.[64]

While it has yet to be determined what role mass spectrometry will play in the routine characterization and analysis of intact viral particles, a glimpse into the potential impact mass spectrometry might have on our understanding of other (and perhaps more fundamentally important macromolecular noncovalent complexes) is offered by recent studies by Robinson and co-workers.[66] In that work intact *E. coli* ribosomes were studies using ESI-TOF instrumentation with a nanoelectrospray ionization source. Individual ions with *m*/*z* in excess of 20 000 were detected and co-added to yield mass spectra of the intact 70S ribosome. Due to the presence of multiple cation adducts, the spectra of the 70S subunit did not afford resolved charge state envelopes, and thus, an a priori mass measurement was not possible. However, based on the partially resolved charge state envelope of the 30S subunit (Figure 5a), a mass measurement of 852 187 ± 3 918 Da was obtained, in good agreement with the theoretical value of 846 681 Da calculated from the combined masses of the 21 small subunit proteins and the 16S RNA. Furthermore, it was shown that while the intact ribosome (70S) was observed from solutions containing 5 mM Mg^{2+} (Figure 5b), the 70S particle was dissociated to its constitutive 50S and 30S subunits if the Mg^{2+} concentration was reduced to 1.7 mM (Figure 5c), consistent with previous solution-phase Mg stability studies. Gas-phase dissociation of the 50S subunit was explored under increasingly harsh interface and collisional activation conditions. The proteins which were most readily dissociated from the 50S subunit were those located at or near the surface and are generally those thought not to have strong interactions with the RNA. It was found that weakly bound proteins were preferentially dissociated from the surface while higher energy collisions lead to successively greater disruption.

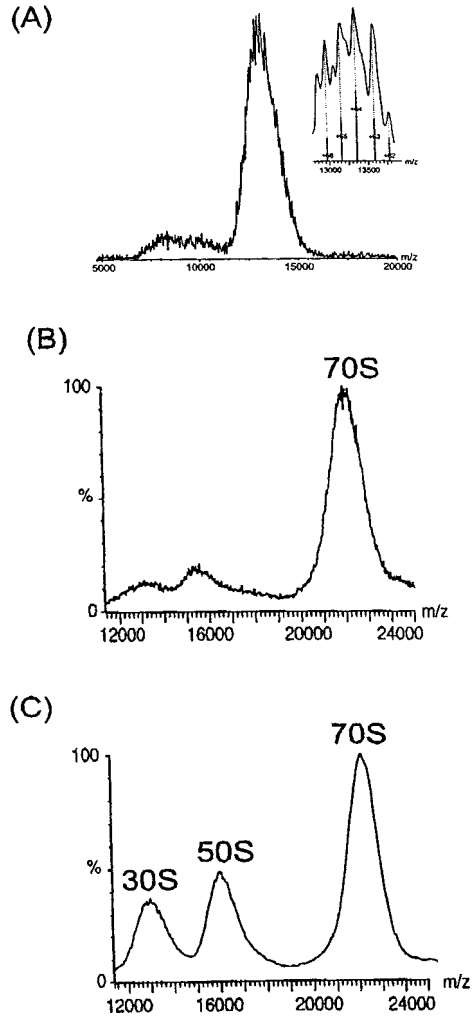

Figure 5. Recent work by Robinson and co-workers highlighting the potential of ESI-MS to study ribosomal subunits and intact ribosomes. (A) Nanoflow ESI-MS of the *E. coli* 30S ribosomal subunit. The partially resolved charge envelope and an iterative error minimization routine yield a mass determination of 852 187 ± 919 Da. (B) ESI-MS analysis of the intact (70S) *E. coli* ribosome from a solution containing 5 mM Mg^{2+}. (C) At 1.7 mM Mg^{2+} the 70S subunit is largely dissociated into the 50S and 30S subunits consistent with previous solution-phase studies. (Adapted with permission from ref 66. Copyright 2000 National Academy of Sciences.)

F. DNA–Drug and Other DNA–Ligand Complexes

Noncovalent interaction of DNA (both single-stranded and duplex) with small molecules provides the basic mechanism of action for a number of therapeutic agents including antitumor, antimicrobial, and antiviral compounds. While a number of analytical schemes have been employed to study these interactions, mass spectrometry is emerging as a powerful technique with which to study such complexes. Early work by Gale and co-workers demonstrated that complexes between a Dickerson-Drew type 12-mer self-complementary DNA duplex and distamycin A, a known minor groove binder, could be effectively analyzed by ESI-MS.[67] As shown in Figure 6, when the ratio of distamycin to duplex was varied, a 1:1 distamycin:DNA complex was observed at low distamycin concentration while a 2:1 distamycin:DNA complex was observed at higher distamycin concentration. These observations are consistent with NMR results for the same sequence and measured distamycin:DNA molar ratios. In a follow up paper, Gale and Smith explored the interaction of several minor groove binders (distamycin A, pentamidine, and Hoechst 33258) with the same self-complementary duplex.[68] Collisionally activated dissociation was used to probe the gas-phase stabilities of the various DNA−drug complexes in an attempt to determine whether differences in solution phase K_d's were reflected in their gas-phase stabilities. The stability of the 2:1 distamycin:DNA complex was found to be greater than that of the 1:1 complex, and it was found that the unbound duplex dissociated more readily than any of the three DNA−drug complexes studied. These findings, and subsequent work employing high-resolution ESI−FTICR MS measurements,[69] set the stage for other researchers interested in MS interrogation of DNA-drug complexes.

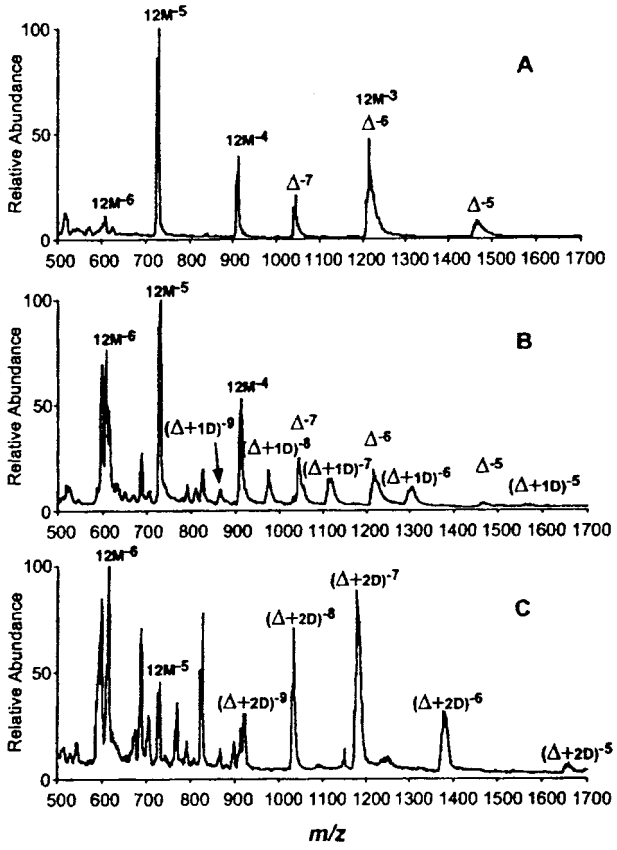

Figure 6. Negative-ion electrospray mass spectra from Gale and co-workers' 1994 paper[67] showing ESI mass spectra of a solution containing 20 μM of the self-complementary oligonucleotide d(CGCAAATTTGCG) with different concentrations of distamycin (Dm). Peaks labeled 12M represent the single-stranded oligo, Δ represents the duplex, (Δ + 1D) represents the 1:1 distamycin:DNA complex, and (Δ + 2D) represents the 2:1 distamycin:DNA complex: (A) no distamycin, (B) 5 μM distamycin, and (C) 20 μM distamycin. Note that the 2:1 binding stoichiometry is favored at higher Dm concentrations. (Reprinted with permission from ref 67. Copyright 1994 American Chemical Society.)

The model systems presented by Gale and Smith were adopted by several other researchers due to their robustness and broad availability of compounds. A paper by Triolo and co-workers[70] essentially re-

peated the early distamycin studies of Gale and Smith, which used a 13 base pair self-complementary oligonucleotide d(CGCGAAATTTGCG)$_2$, using instead a 12 base pair self-complementary d(CGCGAATTCGCG)$_2$. In that work concentration-dependent 1:1 and 2:1 distamycin:DNA complexes were also observed; holding the duplex concentration at 40 μM and titrating the distamycin yielded primarily the 2:1 distamycin:DNA complex at distamycin concentrations $\geq$80 μM. Despite the low signal-to-noise of the spectra shown in that work, the authors were able to evaluate the binding of a series of distamycin derivatives under competitive and noncompetitive binding conditions. It was shown that, in general, derivatives with three pyrrole units had a lower tendency to form 2:1 complexes than those with four pyrrole units—an observation the authors attributed to greater minor groove distortion induced by the longer derivatives. Additionally, the authors unsuccessfully attempted to characterize a complex between daunorubicin and a six base pair self-complimentary oligonucleotide and attributed the failure to the purported poor gas-phase stability of the d(CGATCG)$_2$ duplex. Subsequent work by Wan and coworkers employed the same duplex for the ESI-MS analysis of a collection of minor groove binders and intercalators[71] (see below).

Gabelica and co-workers[34,72] recently used ESI-MS to study the interaction of double-stranded DNA with two classes of antitumor drugs: intercalators (ethidium bromide, amsacrine, and ascididemin) and minor groove binders (distamycin A, Hoechst, netropsin, berenil, and DAPI). The mass spectra suggested that while the minor groove binders bound with specificity and a discrete stoichiometry, the complexes observed with the intercalators exhibited a range of binding stoichiometries consistent with nonspecific binding. Interestingly, the MS-measured abundance of the intercalator:DNA complexes paralleled the polarity of the intercalator; the complexes with ethidium bromide (positively charged) were observed at significantly higher abundance than the complexes with amsacrine (polar) or ascididemin (quasi nonpolar). The relative affinity of the minor groove binders was explored via competitive binding experiments yielding a relative affinity scale of netropsin > distamycin > DAPI > Hoechst 33258 > berenil. Additionally, the preferential stoichiometries of the minor groove binders was determined analyzing solutions with varying ligand concentrations. Consistent with previous studies, distamycin A was observed to preferentially adopt a 2:1 complex at higher concentrations while both Hoechst 33258 and DAPI preferentially adopted a 1:1 complex (some 2:1 was observed at higher concentrations). Only 1:1 complexes were observed for netropsin and berenil.

Kapur and co-workers evaluated the binding of two intercalators, daunomycin and nogalamycin, to a collection of self-complementary oligonucleotides using ESI-MS and noted an oligonucleotide length dependency on the maximum number of ligands bound to a given target.[73] For example, an eight base pair duplex in the presence of a 5-fold molar excess of intercalators gave ESI-MS spectra dominated by species with three ligands bound to each duplex while the 12 base pair duplex contained up to four nogalamycin molecules and six daunomycins. The authors concluded that the observed length-dependent binding stoichiometry is consistent with the neighbor exclusion principle, which states that intercalation occurs between every other base pair. Accordingly, it would be predicted that an *n* base pair duplex could bind as many as *n/2* intercalating molecules.

A recent paper by Wan and co-workers employed ESI-MS to assess the relative affinities and binding stoichiometries of a collection of 10 DNA-binding drugs for a series of self-complementary oligodeoxynucleotides with different GC content ranging in size from 6 to 12 base pairs.[71] Competitive binding experiments with a series of minor groove binders against the 12 base pair self-complementary duplex d(CGCAAATTTGCG)$_2$ yielded a relative affinity rank of Hoechst 33342 > Hoechst 33258 > distamycin > berenil. Note that while the relative affinities of Hoechst 33258 and distamycin A are reversed compared to those determined by Gabelica and coworkers,[34] both studies concluded that berenil has a significantly lower affinity than either Hoechst 33258 or distamycin A. It is worthy of note that while both the Wan and the Gabelica studies employed analogues of the 12 base pair Dickerson dodecamer as a target duplex, a slightly different sequence was employed (Wan used d(CGCAAATTTGCG)$_2$, while Gabelica used a duplex comprised of 5′-GGGGATATGGGG-3′ and its complement). Noncompetitive binding studies revealed approximately a 3-fold improvement in binding of distamycin A to d(CGCGAATTCGCG)$_2$ relative to d(GCGAAATTTCGC)$_2$, while Hoechst 33258 showed no significant sequence-dependent binding affinity. Thus, it is not clear whether the apparent discrepancy in MS-derived relative binding affinities of distamycin A and Hoechst 33258 are the result of the different duplex sequences or whether other variables such as differences in electrospray source design, solution composition, or compound purity are responsible for these contradictory results. Consistent with previous reports by Gale,[67,68] Triolo,[74] and Gabelica,[34] distamycin A was found to bind to the target oligonucleotide with both 1:1 and 2:1 binding stoichiometry. The mode of binding of several compounds was investigated by determining whether the compound bound with higher affinity to a d(ATATAT)$_2$ or a d(GCGCGC)$_2$ target. Distamycin A and berenil exhibited a higher affinity for the AT-rich construct, consistent with operation as minor groove binders. Actinomycin D showed a clear preference for binding to the GC-rich construct, consistent with binding as an intercalator; both of the Hoechst compounds bound comparably to the AT-rich and the GC-rich constructs, suggesting that they operate in a mixed binding mode. Owing to the wealth of information obtained (e.g., relative binding affinities, binding stoichiometry, mode of binding, etc.), the authors suggest that ESI-MS screening strategies have the potential to serve as a powerful platform on which to screen large numbers of compounds against DNA drug targets. On the basis of the level of sophistication of recently presented

automated high-throughput ESI-FTICR-MS-based drug discovery strategies for RNA targets[75,76] (see below), it is highly likely that these predictions will be realized in the coming years.

While the majority of ESI-MS studies of DNA−drug complexes have studied duplex DNA, a few examples have been recently published in which noncovalent complexes between single-stranded DNA and small molecules have been studied.[77] For example, Pócsfalvi and co-workers studied the interaction of a single-stranded 14-mer oligonucleotide with beauvericin mycotoxin using ESI-MS.[78] It was shown that beauvericin binds in a sequence-nonspecific manner and can form complexes with four or more beauvericins bound at higher ligand concentration. As an affinity control, a competitive binding study was conducted between beauvericin and nigericin, another K^+ ionophore. No complexes were observed between the single-strand DNA target and nigericin, while the spectrum was dominated by beauvericin−DNA complexes. Gao and co-workers studied the binding specificity of two similar derivatives of a post-activated neocartzinostatin chromophore to a structured 22-mer bulged-base stem-loop DNA construct.[79] A high degree of binding selectivity was observed between two drug analogues which differed at a single functional group. The R = H compound bound with high affinity at a 1:1 stoichiometry to the target DNA, while no complexes were observed with the R = CH_2OH compound. Neither compound exhibited a significant binding affinity for 19 base pair or 12 base pair control constructs. Finally, Wu and co-workers used tandem mass spectrometry to map the binding sites of metal ions on single-stranded oligonucleotides.[80] 8-mer and 12-mer oligonucleotides were electrosprayed from solutions containing Na^+, Mg^{2+}, and UO_2^{2+} salts, and the resulting oligonucleotide−metal complexes were interrogated by ESI−FTICR-MS. The preferred binding sites of the cations was determined by fragmenting the oligonucleotide−metal complexes and comparing the abundance of metal-adducted and nonadducted fragments. For the 12-mer d(TTGGCCCCTCCTT) oligonucleotide the overall fragmentation pattern was not significantly changed by the addition of the metal ions. Metal ions did not bind appreciably to the terminal TT segments but instead bound preferentially in the vicinity of the central thymine. UO_2^{2+} bound exclusively to the seventh and eighth phosphodiester groups, while Mg^{2+} binding was more delocalized. The authors concluded that metal ion binding to oligonucleotides has both a site and sequence dependence and that such information can be derived directly from high-performance tandem MS measurements.

G. RNA–Ligand Complexes

1. TAR RNA

The transactivation responsive element (TAR) of human immunodeficiency virus type I (HIV-1) adopts a stem−loop secondary structure containing a three-nucleotide bulge flanked by two double-stranded stems. Both the bulge and loop are recognized by protein partners. Mei and co-workers identified three ligands that bind to TAR RNA at different positions.[58] The binding stoichiometry and relative binding affinity for each of the three ligands was determined using ESI-MS. The site of binding for one ligand was isolated in a second ESI-MS experiment. The wild-type 31mer TAR and a modified RNA containing a poly(ethylene glycol) linker instead of the six base loop were co-mixed with the ligand. Only signal from the TAR−ligand complex was observed in the ESI-MS experiment. Loo et al. used ESI-MS to observe a ternary complex formed between TAR, neomycin, and "drug Y" (2,4,5,6-tetraamonoquinazoline) that binds to the upper loop.[81] In-source CAD of the ternary complex resulted in selective loss of the neutral drug Y rather than neomycin, consistent with the difference in their relative affinities for TAR.

Sannes-Lowery et al. studied the binding of neomycin and streptomycin to TAR RNA and the tat−TAR protein−RNA complex.[56] Three neomycin molecules bound sequentially to TAR at increasing concentrations, while only two neomycin molecules bound to the tat−TAR complex. Previous solution-phase studies had failed to demonstrate the binding stoichiometry. The relative affinities of neomycin for TAR were determined in both positive and negative ionization modes. In both cases, neomycin molecules bound sequentially (at similar concentrations) up to a maximum of three bound per TAR. The competitive binding of neomycin and streptomycin to TAR was also evaluated in positive and negative ionization modes. Streptomycin binding to TAR was not observed in the presence of neomycin, although streptomycin alone bound to TAR. The ESI-MS results were consistent with gel shift assays where streptomycin bound TAR with 10-fold lower affinity.

2. 16S A-site RNA

The decoding region of the 16S ribosomal RNA contains a smaller subdomain (**16S**) that folds and retains the key structural features of the full-length RNA.[82] This subdomain binds aminoglycosides at the same location as the intact rRNA. NMR structures have been determined for **16S**-paromomycin and **16S**-gentamicin complexes.[83,84]

Sannes-Lowery et al. used ESI-MS to determine the solution dissociation constants (K_D) and binding stoichiometry for tobramycin and paromomycin with **16S**.[85] Two nonequivalent **16S** binding sites were observed for tobramycin with **16S**, which allowed the proper binding model to be employed in the calculation of the K_D values. They examined the effect of solution conditions such as organic solvent and buffer concentration on the measured tobramycin-**16S** K_D values. Decreasing the buffer concentration 3-fold weakened K_{D2} but did not alter K_{D1}. The K_D measurement for paromomycin-**16S** was not influenced by the amount of organic solvent over a range of 20−50 vol %. The authors also compared two methods for estimating the K_D value: holding the concentration of the ligand fixed and holding the concentration of the RNA fixed. The calculated K_D values differed as did K_D values determined at high and low concentrations of **16S**. This paper highlights the unique information provided by direct observation of nonco-

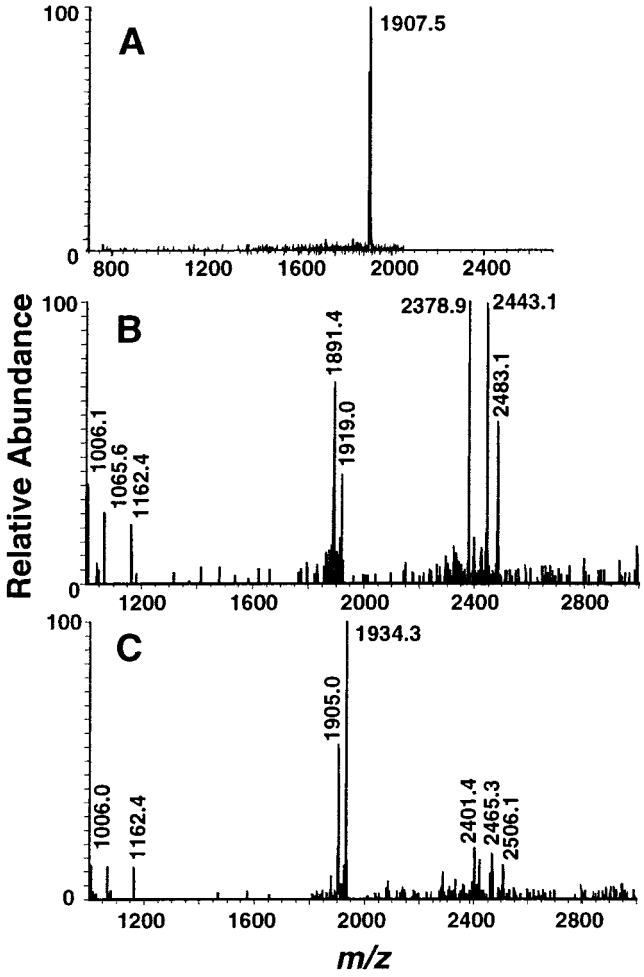

Figure 7. Collisional activation of 16S-ligand complexes at a fixed collision energy. The 16S used in these studies is a chimera containing 3 dA residues at which preferential fragmentation is observed (see text). (A) Collisional activation of the 16S-paromomycin complex at *m*/*z* 1907.5. No fragmentation was observed for ions from the complex with the aminoglycoside under these conditions. (B) The noncovalent complex at *m*/*z* 1919, which is the result of a 676 Da ligand binding to 16S, is collisionally activated under the same conditions as panel A. Substantial fragmentation at the three deoxyadenosine sites is observed. (C) Collisional activation of the noncovalent complex at 1934.3. The three dA sites are protected from fragmentation by the binding of the 735 Da ligand.

valent complexes by ESI-MS and suggests that K_D values are more accurate than solution K_D values measured using indirect detection schemes.

Hofstadler and co-workers demonstrated that binding of five aminoglycosides to **16S** and the human RNA counterpart (**18S**) could be measured in parallel using ESI−FTICR MS.[86] Because the unmodified RNAs differed in mass by only 15 Da, the human RNA subdomain was covalently linked to a poly(ethylene glycol) chain. This neutral mass tag shifted the observed *m*/*z* of the ions to a resolved region of the mass spectrum without altering the ionization properties or ligand binding properties of the RNA. The neomycin-class aminoglycosides bound selectively with high affinity to **16S**, while the kanamycin-class compounds bound to both RNAs with reduced affinity. The mass tag allowed binding of ligands to a control RNA and a target RNA to be studied

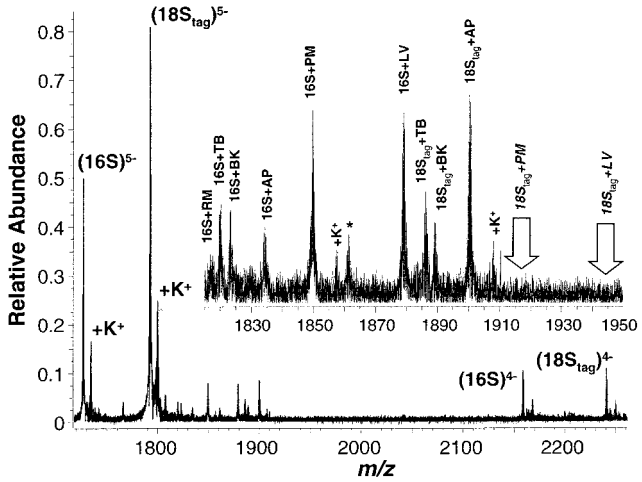

Figure 8. ESI-FTICR-MS spectrum obtained from a mixture of six aminoglycosides (500 nM each) and two 27mer RNAs (5 μM each). Strong signals are observed from the $[M - 4H^+]^{4-}$ and $[M - 5H^+]^{5-}$ ions of the respective 16S and 18S RNA subdomains. Signals from the noncovalent complexes between the RNA and aminoglycosides are shown in the insert. Nearly all of the paromomycin and lividomycin bind to 16S, while no binding is observed to 18S. In contrast, apramycin binds strongly to 18S and only weakly to 16S.

simultaneously under identical solution conditions and ligand concentrations.

Griffey et al. used CAD to study the binding sites of ligands with a modified **16S**.[38] Synthetic incorporation of deoxynucleotides at three positions in a 2′-*O*-methyl version of **16S** was shown to create "weak links" which could be cleaved preferentially with low-power CAD. Binding of paromomycin to the chimeric oligonucleotide resulted in complete protection of the RNA from fragmentation, and the aminoglycoside remained bound to the chimera during the collisional activation period. The modified **16S** was mixed with a 216 member combinatorial library, and ions from two different noncovalent complexes were isolated. As shown in Figure 7a, CAD of the paromomycin complex yielded no fragmentation, while CAD of the complex between **16S** and a compound with mass 676 Da (Figure 7b) resulted in extensive fragmentation at the three deoxy-labeled sites. The masses of the fragments containing the loop of **16S** were shifted by the mass of the bound ligand. CAD of the complex between **16S** and a ligand with mass 753 Da (Figure 7c) produced a different pattern, with significant protection at the three labeled sites and a modest loss of neutral adenine. The library containing the latter compound inhibited an in vitro translation assay, consistent with ligand binding at the ribosomal A site.

Griffey et al. combined ESI−FTICR MS measurements of ligand binding affinity with IRMPD to study the determinants of aminoglycoside binding specificity with sequence variants of **16S**.[76] The binding affinities of six aminoglycosides for **16S** and seven sequence variants were measured in parallel. Paromomycin and lividomycin demonstrated complete binding selectivity for **16S** over **18S**, while apramycin bound to **18S** preferentially (Figure 8). Single base substitutions produced a 200-fold decrease in the

binding affinity between different RNAs. In addition, generation of a G:A mismatch base pair altered the binding specificity of the RNA for tobramycin compared to paromomycin. The **16S** binding sites for paromomycin and ribostamycin were determined using IRMPD as a gas-phase protection assay. The abundances of fragment ions from around the RNA binding site were compared for the free RNA and the respective aminoglycoside complexes. Decreases in the relative amount of fragmentation were observed at three nucleotides in the paromomycin complex, consistent with specific paromomycin−RNA contacts revealed in the NMR structure of the complex.[87,88] Hence, the results from the MS-based protection assay were consistent with the known solution structure. The protection pattern observed for the ribostamycin-**16S** complex had two major differences. The fragmentation of G1405 was lost and the fragmentation at C1407 enhanced. In the NMR structure, G1405 makes a direct contact with ring D of paromomycin while ribostamycin lacks ring D and cannot protect G1405. The enhanced fragmentation at C1407 is consistent with a different binding mode for ribostamycin compared to paromomycin, which may explain the reduced affinity for **16S**.

III. Future Directions

The preponderance of experimental data shows that electrospray ionization transports nucleic acids and their noncovalent complexes into the gas phase with structures and stoichiometries representative of their solution counterparts.[89] Hence, it should prove possible to measure activation energies for gas-phase dissociation of such complexes.[90] Gas-phase H/D exchange or ion mobility measurements of electrosprayed ions may allow differentiation of structural isoforms.[91] Applications of ESI-MS for estimation of protein−nucleic acid and transcription factor−DNA binding stoichiometries should continue to expand, given the importance of such interactions in regulating rates of gene expression and translation. In the majority of studies summarized in this review, the authors offered supporting evidence (in the form of gel-shift assays, NMR studies, chromatography results, etc.) to validate their findings with respect to binding stoichiometry, specificity, and/or affinity. As the body of literature reporting agreement between ESI-MS derived and "conventionally" derived macromolecular properties grows, so too should the confidence in the validity of the measurements. Thus, in the very near future, ESI-MS measurement of the biophysical properties of noncovalent complexes will stand on their own merit and not need confirmation using other techniques. ESI-MS has emerged as a very powerful tool for early-stage drug discovery, and identification of novel antiviral and antimicrobial compounds should result in the near term. ESI-MS will play an important role in understanding the assembly and function of biological nucleic acid−protein machines such as the transcriptional apparatus, the ribosome, and the spliceosome, since the stoichiometry and order of protein binding can be ascertained based on the masses of the observed complexes.

IV. Acknowledgments

We thank all of our co-workers whose efforts have made much of this work possible. This work was funded in part by DARPA grant N65236-99-1-5419 and Department of Commerce ATP grant 97-01-0135.

V. References

(1) Ganem, B.; Li, Y.-T.; Henion, J. D. *J. Am. Chem. Soc.* **1991**, *113*, 6294.
(2) Fenn, J. B.; Mann, M.; Meng, C. K.; Wong, S. F.; Whitehouse, C. M. *Science* **1989**, *246*, 64.
(3) Winger, B. E.; Light-Wahl, K. J.; Rockwood, A. L.; Smith, R. D. *J. Am. Chem. Soc.* **1992**, *114*, 5897.
(4) Mirza, U. A.; Cohen, S. L.; Chait, B. T. *Anal. Chem.* **1993**, *65*, 1.
(5) Smith, R. D.; Light-Wahl, K. J.; Winger, B. E.; Loo, J. A. *Org. Mass Spectrom.* **1992**, *27*, 811.
(6) Loo, J. A. *Bioconjugate Chem.* **1995**, *6*, 644.
(7) Loo, J. A. *Mass Spectrom. Rev.* **1997**, *16*, 1.
(8) Bruce, J. E.; Anderson, G. A.; Chen, R. D.; Cheng, X. H.; Gale, D. C.; Hofstadler, S. A.; Schwartz, B. L.; Smith, R. D. *Rapid Commun. Mass Spectrom.* **1995**, *9*, 644.
(9) Ecker, D. J.; Griffey, R. H. *Drug Discovery Today* **1999**, *4*, 420.
(10) Crain, P. F.; McCloskey, J. A. *Curr. Opin. Biotechnol.* **1998**, *9*, 25.
(11) Nordhoff, E. *TRAC−Trends in Analytical Chemistry* **1996**, *15*, 240.
(12) Nordhoff, E.; Kirpekar, F.; Roepstorff, P. *Mass Spectrom. Rev.* **1996**, *15*, 67.
(13) Bahr, U.; Karas, M.; Hillenkamp, F. *Fresenius' J. Anal. Chem.* **1994**, *348*, 783.
(14) Bakhtiar, R.; Hofstadler, S.; Muddiman, D.; Smith, R. *J. Chem. Educ.* **1997**, *74*, 1288.
(15) Spengler, B.; Kaufmann, R. *ANALUSIS* **1992**, *20*, 91.
(16) Karas, M.; Bahr, U.; Giessmann, U. *Mass Spectrom. Rev.* **1991**, *10*, 335.
(17) Light-Wahl, K. J.; Springer, D. L.; Winger, B. E.; Edmonds, C. G.; Camp, D. G.; Thrall, B. D.; Smith, R. D. *J. Am. Chem. Soc.* **1993**, *115*, 803.
(18) Ganem, B.; Li, Y. T.; Henion, J. D. *Tetrahedron Lett.* **1993**, *34*, 1445.
(19) Doktycz, M. J.; Habibigoudarzi, S.; McLuckey, S. A. *Anal. Chem.* **1994**, *66*, 3416.
(20) Bayer, E.; Bauer, T.; Schmeer, K.; Bleicher, K.; Maler, M.; Gaus, H. J. *Anal. Chem.* **1994**, *66*, 3858.
(21) Greig, M. J.; Gaus, H. J.; Griffey, R. H. *Rapid Commun. Mass Spectrom.* **1996**, *10*, 47.
(22) Cheng, X.; Gao, Q.; Smith, R. D.; Jung, K.-E.; Switzer, C. *Chem. Commun. (Cambridge)* **1996**, 747.
(23) Aaserud, D. J.; Kelleher, N. L.; Little, D. P.; McLafferty, F. W. *J. Am. Soc. Mass Spectrom.* **1996**, *7*, 1266.
(24) Muddiman, D. C.; Wunschel, D. S.; Liu, C.; Pasa-Tolic, L.; Fox, K. F.; Fox, A.; Anderson, G. A.; Smith, R. D. *Anal. Chem.* **1996**, *68*, 3705.
(25) Naito, Y.; Ishikawa, K.; Koga, Y.; Tsuneyoshi, T.; Terunuma, H. *Rapid Commun. Mass Spectrom.* **1995**, *9*, 1484.
(26) Wunschel, D. S.; Fox, K. F.; Fox, A.; Bruce, J. E.; Muddiman, D. C.; Smith, R. D. *Rapid Commun. Mass Spectrom.* **1996**, *10*, 29.
(27) Muddiman, D. C.; Null, A. P.; Hannis, J. C. *Rapid Commun. Mass Spectrom.* **1999**, *13*, 1201.
(28) Cheng, X.; Camp, D. G. I.; Wu, Q.; Bakhtiar, R.; Springer, D. L.; Morris, B. J.; Bruce, J. E.; Anderson, G. A.; Edmonds, C. G.; Smith, R. D. *Nucleic Acid Res.* **1996**, *24*, 2183.
(29) Chen, R.; Cheng, X.; Mitchell, D. W.; Hofstadler, S. A.; Wu, Q.; Rockwood, A. L.; Sherman, M. G.; Smith, R. D. *Anal. Chem.* **1995**, *67*, 1159.
(30) Aaserud, D. J.; Guan, Z.; Little, D. P.; McLafferty, F. W. *Int. J. Mass Spectrom. Ion Processes* **1997**, *167*, 705.
(31) McLafferty, F. W.; Aaserud, D. J.; Guan, Z.; Little, D. P.; Kelleher, N. L. *Int. J. Mass Spectrom. Ion Processes* **1997**, *165*, 457.
(32) Little, D. P.; Aaserud, D. J.; Valaskovic, G. A.; McLafferty, F. W. *J. Am. Chem. Soc.* **1996**, *118*, 9352.
(33) Little, D. P.; Speir, J. P.; Senko, M. W.; O'Connor, P. B.; McLafferty, F. W. *Anal. Chem.* **1994**, *66*, 2809.
(34) Gabelica, V.; De Pauw, E.; Rosu, F. *J. Mass Spectrom.* **1999**, *34*, 1328.
(35) Wan, K. X.; Shibue, T.; Gross, M. L. *J. Am. Chem. Soc.* **2000**, *122*, 300.
(36) Schnier, P. D.; Klassen, J. S.; Strittmatter, E. F.; Williams, E. R. *J. Am. Chem. Soc.* **1998**, *120*, 9605.
(37) Griffey, R. H.; Greig, M. J. *Proc. SPIE-Int. Soc. Opt. Eng.* **1997**, *2985*, 82.
(38) Griffey, R. H.; Greig, M. J.; An, H.; Sasmor, H.; Manalili, S. *J. Am. Chem. Soc.* **1999**, *121*, 474.

(39) McLuckey, S. A.; Habibigoudarzi, S. *J. Am. Chem. Soc.* **1993**, *115*, 12085.
(40) Robinson, J. M.; Greig, M. J.; Griffey, R. H.; Mohan, V.; Laude, D. A. *Anal. Chem.* **1998**, *70*, 3566.
(41) Griffey, R. H.; Greig, M. J.; Robinson, J. M.; Laude, D. A. *Rapid Commun. Mass Spectrom.* **1999**, *13*, 113.
(42) Freitas, M. A.; Shi, S. D.-H.; Hendrickson, C. L.; Marshall, A. G. *J. Am. Chem. Soc.* **1998**, *120*, 10187.
(43) Greig, M.; Robinson, J.; Laude, D.; Griffey, R. The 45th ASMS Conference on Mass Spectrometry and Allied Topics, Palm Springs, CA, 1997.
(44) Hofstadler, S. A.; Sannes-Lowery, K. A.; Griffey, R. H. *J. Mass Spectrom.* **1999**, *35*, 62.
(45) Griffith, M. C.; Risen, L. M.; Greig, M. J.; Lesnik, E. A.; Sprankle, K. G.; Griffey, R. H.; Kiely, J. S.; Freier, S. M. *J. Am. Chem. Soc.* **1995**, *117*, 831.
(46) Goodlett, D. R.; Camp, D. G.; Hardin, C. C.; Corregan, M.; Smith, R. D. *Biol. Mass Spectrom.* **1993**, *22*, 181.
(47) Greig, M. J.; Gaus, H.; Cummins, L. L.; Sasmor, H.; Griffey, R. H. *J. Am. Chem. Soc.* **1995**, *117*, 10765.
(48) Crooke, S. T.; Graham, M. J.; Zuckerman, J. E.; Brooks, D.; Conklin, B. S.; Cummins, L. L.; Greig, M. J.; Guinosso, C. J.; Kornburst, D.; Manoharan, M.; Sasmor, H. M.; Schleich, T.; Tivel, K. L.; Griffey, R. H. *J. Pharmacol. Exp. Ther.* **1996**, *277*, 923.
(49) Cheng, X.; Morin, P. E.; Harms, A. C.; Bruce, J. E.; Ben-David, Y.; Smith, R. D. *Anal. Biochem.* **1996**, *239*, 35.
(50) Cheng, X.; Harms, A. C.; Goudreau, P. N.; Terwilliger, T. C.; Smith, R. D. *Proc. Natl. Acad. Sci. U.S.A.* **1996**, *93*, 7022.
(51) Cheng, X.; Hofstadler, S. A.; Bruce, J. E.; Harms, A. C.; Chen, R.; Smith, R. D.; Terwilliger, T. C.; Goudreau, P. N. In *Techniques Protein Chemistry VII*, *[Symp. Protein Soc.], 9th*; Marshak, D. R., Ed.; Academic: San Diego, CA, 1996; p 13.
(52) Veenstra, T. D.; Benson, L. M.; Craig, T. A.; Tomlinson, A. J.; Kumar, R.; Naylor, S. *Nat. Biotechnol.* **1998**, *16*, 262.
(53) Potier, N.; Donald, L. J.; Chernushevich, I.; Ayed, A.; Ens, W.; Arrowsmith, C. H.; Standing, K. G.; Duckworth, H. W. *Protein Sci.* **1998**, *7*, 1388.
(54) Xu, N.; Pasa-Tolic, L.; Smith, R. D.; Ni, S.; Thrall, B. D. *Anal. Biochem.* **1999**, *272*, 26.
(55) Sannes-Lowery, K. A.; Hu, P.; Mack, D. P.; Mei, H.-Y.; Loo, J. A. *Anal. Chem.* **1997**, *69*, 5130.
(56) Sannes-Lowery, K. A.; Mei, H.-Y.; Loo, J. A. *Int. J. Mass Spectrom.* **1999**, *193*, 115.
(57) Loo, J. A.; Sannes-Lowery, K. A.; Hu, P.; Mack, D. P.; Mei, H.-Y. In *New Methods for the Study of Biomolecular Complexes*; Ens, W., Standing, K. G., Chernushevich, I. V., Eds.; Kluwer: Dordrecht, 1998; Vol. 510, p 83.
(58) Mei, H. Y.; Cui, M.; Heldsinger, A.; Lemrow, S. M.; Loo, J. A.; Sannes-Lowery, K. A.; Sharmeen, L.; Czarnik, A. W. *Biochemistry* **1998**, *37*, 14204.
(59) Mei, H.-Y.; Mack, D. P.; Galan, A. A.; Halim, N. S.; Heldsinger, A.; Loo, J. A.; Moreland, D. W.; Sannes-Lowery, K. A.; Sharmeen, L.; Truong, H. N.; Czarnik, A. W. *Bioorg. Med. Chem.* **1997**, *5*, 1173.
(60) Liu, C.; Tolic, L. P.; Hofstadler, S. A.; Harms, A. C.; Smith, R. D.; Kang, C.; Sinha, N. *Anal. Biochem.* **1998**, *262*, 67.
(61) Gauthier, J. W.; Trautman, T. R.; Jacobson, D. B. *Anal. Chim. Acta* **1991**, *246*, 211.
(62) Siuzdak, G.; Bothner, B.; Yeager, M.; Brugkdou, C.; Faquet, C. M.; Hoey, K.; Chang, C. M. *Chem. Biol.* **1996**, *3*, 45.
(63) Siuzdak, G. *J. Mass Spectrom.* **1998**, *33*, 203.
(64) Chernushevich, I. V.; Ens, W.; Standing, K. G. In *New Methods for the Study of Biomolecular Complexes*; Ens, W., Standing, K. G., Chernushevich, I. V., Eds.; Kluwer Academic Publishers: Dordrecht, 1998; Vol. 510, p 101.
(65) Tito, M. A.; Tars, K.; Valegard, K.; Hadju, J.; Robinson, C. V. *J. Am. Chem. Soc.* **2000**, *122*, 3550.
(66) Rostom, A. A.; Fucini, P.; Benjamin, D. R.; Juenemann, R.; Nierhaus, K. H.; Hartl, F. U.; Dobson, C. M.; Robinson, C. V. *Proc. Natl. Acad. Sci. U. S. A.* **2000**, *97*, 5185.
(67) Gale, D. C.; Goodlett, D. R.; Light-Wahl, K. J.; Smith, R. D. *J. Am. Chem. Soc.* **1994**, *116*, 6027.
(68) Gale, D. C.; Smith, R. D. *J. Am. Soc. Mass Spectrom.* **1995**, *6*, 1154.
(69) Smith, R. D.; Cheng, X.; Schwartz, B. L.; Chen, R.; Hofstadler, S. A. *ACS Symp. Ser.* **1996**, *619*, 294.
(70) Triolo, A.; Arcamone, F. M.; Raffaelli, A.; Salvadori, P. *J. Mass Spectrom.* **1997**, *32*, 1186.
(71) Wan, K. X.; Shibue, T.; Gross, M. L. *J. Am. Chem. Soc.* **2000**, *122*, 300.
(72) Gabelica, V.; Rosu, F.; Houssier, C.; De Pauw, E. *Rapid Commun. Mass Spectrom.* **2000**, *14*, 464.
(73) Kapur, A.; Beck, J. L.; Sheil, M. M. *Rapid Commun. Mass Spectrom.* **1999**, *13*, 2489.
(74) Schuster, S.; Fell, D. A.; Dandekar, T. *Nat. Biotechnol* **2000**, *18*, 326.
(75) Sannes-Lowery, K. A.; Drader, J. J.; Griffey, R. H.; Hofstadler, S. A. *TrAC, Trends Anal. Chem.* **2000**, *19*, 481.
(76) Griffey, R. H.; Hofstadler, S. A.; Sannes-Lowery, K. A.; Ecker, D. J.; Crooke, S. T. *Proc. Natl. Acad. Sci. U.S.A.* **1999**, *96*, 10129.
(77) Beck, J. L.; Humphries, A.; Sheil, M. M.; Ralph, S. F. *Eur. Mass Spectrom.* **1999**, *5*, 489.
(78) Pocsfalvi, G.; Dilanda, G.; Ferranti, P.; Ritieni, A.; Randazzo, G.; Malorni, A. *Rapid Commun. Mass Spectrom.* **1997**, *11*, 265.
(79) Gao, Q.; Cheng, X.; Smith, R. D.; Yang, C. F.; Goldberg, I. H. *J. Mass Spectrom.* **1996**, *31*, 31.
(80) Wu, Q.; Cheng, X.; Hofstadler, S. A.; Smith, R. D. *J. Mass Spectrom.* **1996**, *31*, 669.
(81) Loo, J. A.; Thanabal, V.; Mei, H.-Y. *Mass Spectrom. Biol. Med.* **2000**, 73.
(82) Purohit, P.; Stern, S. *Nature* **1994**, *370*, 659.
(83) Fourmy, D.; Recht, M. I.; Blanchard, S. C.; Puglisi, J. D. *Science (Washington, D.C.)* **1996**, *274*, 1367.
(84) Yoshizawa, S.; Fourmy, D.; Puglisi, J. D. *EMBO J.* **1998**, *17*, 6437.
(85) Sannes-Lowery, K. A.; Griffey, R. H.; Hofstadler, S. A. *Anal. Biochem.* **2000**, *280*, 264.
(86) Hofstadler, S. A.; Sannes-Lowery, K. A.; Crooke, S. T.; Ecker, D. J.; Sasmor, H.; Manalili, S.; Griffey, R. H. *Anal. Chem.* **1999**, *71*, 3436.
(87) Fourmy, D.; Recht, M. I.; Puglisi, J. D. *J. Mol. Biol.* **1998**, *277*, 347.
(88) Fourmy, D.; Yoshizawa, S.; Puglisi, J. D. *J. Mol. Biol.* **1998**, *277*, 333.
(89) Wang, F.; Freitas, M. A.; Marshall, A. G.; Sykes, B. D. *Int. J. Mass Spectrom.* **1999**, *192*, 319.
(90) Freitas, M. A.; Hendrickson, C. L.; Marshall, A. G. *Rapid Commun. Mass Spectrom.* **1999**, *13*, 1639.
(91) Valentine, S. J.; Clemmer, D. E. *J. Am. Chem. Soc.* **1997**, *119*, 3558.

CR990105O